Acta Oceanol. Sin., 2020, Vol. 39, No. 12, P. 1–10
https://doi.org/10.1007/s13131-020-1685-y
http://www.hyxb.org.cn
E-mail: hyxbe@263.net

Accuracy assessment of global ocean tide models in the South China Sea using satellite altimeter and tide gauge data

Yanguang Fu[1], Yikai Feng[1]*, Dongxu Zhou[1]*, Xinghua Zhou[1, 2], Jie Li[1], Qiuhua Tang[1]

[1] First Institute of Oceanography, Ministry of Natural Resources, Qingdao 266061, China

[2] College of Geodesy and Geomatics, Shandong University of Science and Technology, Qingdao 266590, China

Received 2 July 2019; accepted 9 April 2020

Abstract

In this study, to meet the need for accurate tidal prediction, the accuracy of global ocean tide models was assessed in the South China Sea (0°–26°N, 99°–121°E). Seven tide models, namely, DTU10, EOT11a, FES2014, GOT4.8, HAMTIDE12, OSU12 and TPXO8, were considered. The accuracy of eight major tidal constituents (i.e., Q_1, O_1, P_1, K_1, N_2, M_2, S_2 and K_2) were assessed for the shallow water and coastal areas based on the tidal constants derived from multi-mission satellite altimetry (TOPEX and Jason series) and tide gauge observations. The root mean square values of each constituent between satellite-derived tidal constants and tide models were found in the range of 0.72–1.90 cm in the deep ocean (depth>200 m) and 1.18–5.63 cm in shallow water area (depth<200 m). Large inter-model discrepancies were noted in the Strait of Malacca and the Taiwan Strait, which could be attributable to the complicated hydrodynamic systems and the paucity of high-quality satellite altimetry data. In coastal regions, an accuracy performance was investigated using tidal results from 37 tide gauge stations. The root sum square values were in the range of 9.35–19.11 cm, with the FES2014 model exhibiting slightly superior performance.

Key words: accuracy assessment, tide model, satellite altimetry, tide gauge, South China Sea

Citation: Fu Yanguang, Feng Yikai, Zhou Dongxu, Zhou Xinghua, Li Jie, Tang Qiuhua. 2020. Accuracy assessment of global ocean tide models in the South China Sea using satellite altimeter and tide gauge data. Acta Oceanologica Sinica, 39(12): 1–10, doi: 10.1007/s13131-020-1685-y

1 Introduction

Ocean tide model is an important element in determining the gravity field, sea surface topography and depth datum models with high accuracy and high resolution. Precise tide models can provide sea level corrections for various measurements, e.g., bathymetry survey data and satellite altimetry data (Fu and Cazenave, 2001; Visser et al., 2010). They can also provide basic data with which to establish accurate vertical datum transformations (Iliffe et al., 2013; Keysers et al., 2015).

Satellite altimeter data and tide gauge observations represent the most effective and direct way in which to evaluate the accuracy of tidal constituents (Shum et al., 1997; Seifi et al., 2019). Considerable insight into large-scale ocean processes has been gained throughout 300 years of oceanographic observations. For example, many numerical tide models that were developed before the advent of satellite altimetry could produce accurate results, although the accuracy of such tide models has been improved during the satellite era. The TOPEX/Poseidon (T/P), Jason-1, Jason-2 and Jason-3 satellites have recorded altimetry data for over 20 years, and the current accuracy of tidal predictions for the open ocean is well over 2 cm (Andersen et al., 1995; Stammer et al., 2014). Compared with the open ocean, altimeter data are geographically diverse in shallow-water areas (Fok et al., 2010). Moreover, they can be affected by environmental factors such as the shoreline and topography (Cherniawsky et al., 2001), and physical factors such as tropospheric and ionospheric correction models (Lyard et al., 2006; Desportes et al., 2007). Mayer-Gürr et al. (2012), Daher et al. (2015), and Cheng et al. (2016) all used the least-squares-based harmonic analysis method on satellite altimetry data of different timescales to obtain along-track tidal constants. Satellite-derived tidal information can play an important role in the establishment of tide models, e.g., providing open boundary conditions with which to establish an assimilation model or as an interpolation resource with which to establish an empirical model.

As a traditional tool for obtaining tidal height, a tide gauge station can provide verifiable, accurate, high-frequency tidal information, particularly along coastlines. However, the main drawback of such measurements is the sparsity of observation locations. Harmonic analysis of tide gauge observations can produce tidal information that is highly accurate to the millimeter level. Recently, the application of tide gauge data has been expanded. For example, they have been applied in establishing tide models and used as ground-truth data with which to assess the accuracy of such models.

The accuracy performance of the global tide models in regional areas, such as the shallow water and coastal zones, is different from their performance in global ocean in terms of the accuracy of tidal constituent estimations and, consequently, the accuracies of tidal height predictions. Stammer et al. (2014) conducted a suite of comprehensive tests of seven modern altimeter-constrained ocean-tide models. Many of the tests relied on com-

Foundation item: The National Key Research and Development Program of China under contract Nos 2017YFC0306003 and 2016YFB0501703; the National Natural Science Foundation of China under contract Nos 41876111, 41706115 and 41806214.
*Corresponding author, E-mail: ykfeng@fio.org.cn; zhoudongxu@fio.org.cn

parisons against *in situ* tidal measurements, but some relied on remote measurements.

The South China Sea (SCS) is a broad marginal sea. The ocean dynamics and tides in this area are complicated, with flows through the Luzon Strait and the complex topography leading to the generation and scattering of interval waves with various frequencies (Egbert and Ray, 2000) and to the existence of a tidal system with several amphidromic systems (Green and David, 2013). In the deep-water area, the tidal system is reasonably simple, whereas, the tidal regimes in the shallow-water areas are complex and the tidal currents can be strong (Ye and Robinson, 1983). Tides in the SCS have been studied for decades (Fang, 1986), with most provides research focused on how best to establish an appropriate numerical model (Fang et al., 1999; Zu et al., 2008). Given the continuous accumulation of satellite altimeter and tide gauge datasets over many years, it is very meaningful to use such information to analyse the accuracy of relevant state-of-the-art tide models.

In this study, the accuracy performance of seven recent empirical and assimilation tidal models were investigated by satellite-derived and tide gauge results in the shallow water and coastal regions of the SCS areas. The remainder of this paper is organized as follows. Descriptions of the datasets and the methodology used are provided in Sections 2 and 3, respectively. Section 4 presents the results of the comparison between tide models and satellite-derived and tide gauge results. Sections 5 and 6 conduct discussions of the accuracy performance difference and the conclusions of the study, respectively.

2 Study area and data

The study area of the SCS is bounded by 0°–26°N, 99°–121°E. Figure 1 shows the bathymetry based on the ETOP1 model available from https://www.ngdc.noaa.gov. This model is a 1 arc-minute global relief model of Earth's surface that integrates land topography and ocean bathymetry, and built from global and regional data sets (Amante and Eakins, 2009).

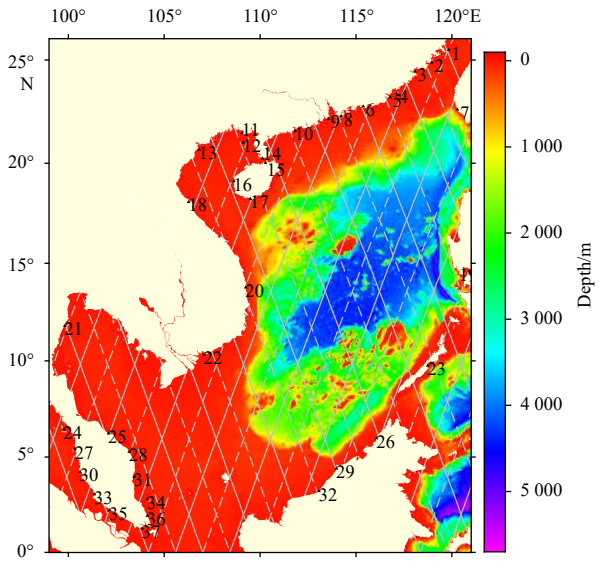

Fig. 1. Distribution of satellite altimetry along-track points and tide gauge stations in the study area. The numbered dark triangles denote the 37 tide gauges. Gray solid and dashed lines are the primary and interleaved mission tracks, respectively.

2.1 *Tide gauge data*

In the SCS area, the tidal constants for this study were obtained from 37 tide gauge observations, of which 27 stations were part of the University of Hawaii Sea Level Center (UHSLC, https://uhslc.soest.hawaii.edu), and the other 10 stations were Chinese long-term tide gauge stations, as shown in Table 1. Tidal height time series of each tide gauge station used in this study comprised hourly tidal height data and acquired over at least 1 year and with a record that was at least 85% complete for the analysis period.

2.2 *Satellite altimetry data*

The along-track tidal constituents of multi-mission satellite altimetry data were obtained from the new Centre for Topographic studies of the Ocean and Hydrosphere (CTOH) tidal constants product (http://ctoh.legos.obs-mip.fr/). The CTOH computes and distributes tidal constants estimated by harmonic analysis of each single time series (i.e., every 6.2 km). The sea level height time series have been computed for the whole TOPEX/Poseidon, Jason-1, Jason-2 and Jason-3 period with primary and interleaved mission data applying the latest reprocessing CTOH standards.

The spatial locations and the record length of the single time series of the tidal estimates along the altimeter ground track were indicated for each constituent. In this study, eight major tidal constituents in the along-track points were extracted from the CTOH primary and interleaved mission tracks, respectively, as shown in Fig. 1.

2.3 *Tide models used*

This study assessed seven global ocean tide models: DTU10, EOT11a, FES2014, GOT4.8, HAMTIDE12, OSU12 and TPXO8. The selected models represent those commonly adopted for eliminating the tidal signal from altimetry measurements. Table 2 presents the resolution, constituents and type of the seven tide models used.

The global ocean tide models adopted in this study can be grouped into two categories: empirical models, which mainly rely on satellite-derived and tide gauge results (OSU12 and GOT4.8), and hydrodynamic model maybe used to analyze the time series of tide residuals (DTU10 and EOT11a); assimilation models (FES2014, HAMTIDE12 and TPXO8) that are constrained using empirical observations through different assimilation approaches. Each model used for the accuracy assessment is as the followings.

DTU10 of the Technical University of Denmark was developed based on an empirical correction to the FES2004 model (Cheng and Andersen, 2011; Lyard et al., 2006). The response method (Groves and Reynolds, 1975; Munk and Cartwright, 1966) is applied to the multi-mission altimeter tide residuals and the dynamic interpolation method is used to perform interpolation of the along-track data to the FES2004 grid. Multi-mission satellite altimeters sea level data were applied to obtain improved global sea level residuals.

EOT11a is a global empirical ocean tide model derived in 2011 through residual analysis of multi-mission satellite altimeter data (Savcenko and Bosch, 2012). The model was computed based on residual tidal analysis of multi-mission altimeter data from the T/P, ERS-2, Envisat, Jason-1 and Jason-2 satellite, acquired between September 1992 and April 2010.

The Goddard/Grenoble Ocean Tide (GOT) empirical model is used widely to remove barotropic ocean tides from satellite altimetry data (Ray, 1999; Schrama and Ray, 1994). The latest ver-

Table 1. The geographical coordinates, time range, amplitude and phase of the four major tidal constituents of the tide gauge stations located in the South China Sea

Station No.	Name	Geographic coordinate	Time coverage	K_1		O_1		M_2		S_2	
				Amplitude/cm	Phase/(°)	Amplitude/cm	Phase/(°)	Amplitude/cm	Phase/(°)	Amplitude/cm	Phase/(°)
1	Pingtan	25.47°N, 119.83°E	2010–2012	30.41	131.19	24.71	99.99	205.32	78.05	62.52	113.20
2	Chongwu	24.88°N, 118.95°E	2010–2012	32.20	148.67	26.29	115.70	206.05	97.93	61.41	137.41
3	Xiamen	24.45°N, 118.07°E	1954–1997	34.16	163.62	27.84	122.47	184.80	120.10	54.01	163.41
4	Nanao	23.40°N, 117.10°E	2010–2012	30.24	169.44	24.94	131.15	56.44	130.59	13.90	187.35
5	Shantou	23.22°N, 116.78°E	2010–2012	29.70	170.54	24.62	131.35	33.71	129.78	6.75	198.40
6	Shanwei	22.77°N, 115.37°E	2010–2012	32.56	177.07	26.47	137.80	27.16	26.72	10.54	38.08
7	Kaohsiung	22.62°N, 120.28°E	1983–2013	17.69	165.86	15.99	129.54	18.14	350.66	6.71	350.90
8	Hong Kong	22.30°N, 114.22°E	1986–2012	35.32	166.96	28.08	121.94	39.50	7.91	15.73	27.55
9	Macau	22.17°N, 113.55°E	1978–1985	37.64	186.97	30.56	146.18	46.36	56.04	18.65	81.29
10	Zhapo	21.58°N, 111.83°E	1975–1997	41.51	195.04	35.13	149.09	64.43	61.61	27.99	92.55
11	Beihai	21.47°N, 109.05°E	2010–2012	90.67	336.14	98.36	281.53	45.47	306.41	11.05	357.97
12	Weizhou	21.02°N, 109.12°E	2010–2012	86.48	333.60	94.59	279.18	38.84	300.59	9.80	354.40
13	Hon Dau	20.67°N, 106.82°E	1960–1960	70.49	92.42	78.40	28.40	5.87	40.88	4.40	104.39
14	Haian	20.23°N, 110.13°E	2010–2012	44.26	329.66	53.67	276.37	16.35	17.28	11.18	79.36
15	Haikou	20.02°N, 110.28°E	1976–1997	37.32	335.62	44.48	281.83	22.50	26.69	12.94	81.45
16	Dongfanggang	19.11°N, 108.63°E	2010–2012	54.25	311.64	63.59	259.50	18.01	190.26	5.71	239.50
17	Sanya	18.23°N, 109.50°E	2010–2012	31.16	209.59	29.49	173.21	21.56	88.74	7.15	121.54
18	Vung Ang	18.08°N, 106.28°E	1996–1997	32.62	98.13	40.48	31.05	24.70	353.50	6.59	62.79
19	Manila	14.58°N, 120.97°E	1984–2012	32.95	198.16	28.87	153.38	19.75	63.84	7.29	95.31
20	Qui Nohn	13.77°N, 109.25°E	1994–2005	32.77	192.81	27.55	153.03	17.72	85.42	6.97	120.66
21	Ko Lak	11.80°N, 99.82°E	1985–2012	51.62	59.48	33.53	17.81	6.44	291.48	1.51	339.18
22	Vung Tau	10.33°N, 107.07°E	1986–2002	63.78	207.34	50.34	166.50	75.39	194.89	29.46	231.06
23	Puerto Princesa	9.75°N, 118.73°E	1998–2012	34.21	204.88	29.88	167.81	29.92	79.78	15.99	113.35
24	Langkawi	6.43°N, 99.77°E	1985–2012	16.70	232.40	5.19	183.55	80.12	118.28	44.48	155.80
25	Geting	6.23°N, 102.10°E	1986–2011	23.81	233.36	12.29	190.06	16.98	20.21	8.11	50.96
26	Kota Kinabalu	5.98°N, 116.07°E	1987–2011	34.78	194.53	30.07	152.82	23.59	88.36	10.20	115.43
27	Penang	5.42°N, 100.35°E	1984–2011	19.56	237.20	5.08	177.45	61.26	152.29	36.13	185.91
28	Cendering	5.27°N, 103.18°E	1984–2011	48.07	238.41	29.50	209.61	30.09	5.98	12.02	42.85
29	Miri	4.40°N, 113.97°E	1992–2011	35.84	194.52	31.35	154.15	17.81	101.45	8.68	123.43
30	Lumut	4.23°N, 100.62°E	1984–2011	21.61	246.33	3.19	159.22	74.47	241.51	34.95	275.77
31	Kuantan	3.98°N, 103.43°E	1983–2011	52.04	254.40	34.81	218.17	52.57	29.86	17.33	68.75
32	Bintulu	3.22°N, 113.07°E	1992–2011	39.80	198.57	32.18	160.95	19.04	182.12	6.02	165.73
33	Kelang	3.05°N, 101.37°E	1983–2011	19.42	264.68	3.50	48.94	137.63	284.38	69.07	325.67
34	Tioman	2.80°N, 104.13°E	1985–2011	46.14	264.23	34.56	231.25	59.16	40.80	18.43	83.16
35	Keling	2.22°N, 102.15°E	1984–2011	9.08	29.94	20.99	34.13	61.13	356.11	29.86	35.40
36	Sedili	1.93°N, 104.12°E	1986–2011	33.28	286.01	28.22	253.65	56.22	59.35	16.06	107.42
37	Tanjong Pagar	1.27°N, 103.85°E	1988–2011	30.61	350.46	29.68	306.02	79.32	91.84	32.14	138.38

Note: Column 1 is the tide gauge number used corresponding to the location in Fig. 1.

Table 2. Main properties of the seven ocean tide models under review

Tide models	Resolution	Major constituents		Type
		Diurnal	Semidiurnal	
DTU10	(1/8)°×(1/8)°	K_1, O_1, P_1, Q_1, S_1	M_2, S_2, N_2, K_2	E
EOT11a	(1/8)°×(1/8)°	K_1, O_1, P_1, Q_1, S_1	M_2, S_2, N_2, K_2, $2N_2$	E
FES2014	(1/16)°×(1/16)°	K_1, O_1, P_1, Q_1, S_1	M_2, S_2, N_2, K_2, $2N_2$	H
GOT4.8	(1/2)°×(1/2)°	K_1, O_1, P_1, Q_1, S_1	M_2, S_2, N_2, K_2	E
HAMTIDE12	(1/8)°×(1/8)°	K_1, O_1, P_1, Q_1	M_2, S_2, N_2, K_2	H
OSU12	(1/4)°×(1/4)°	K_1, O_1, P_1, Q_1, S_1	M_2, S_2, N_2, K_2	E
TPXO8	(1/30)°×(1/30)°	K_1, O_1, P_1, Q_1, S_1	M_2, S_2, N_2, K_2	H

Note: E, empirical adjustment to an adopted prior model; H, assimilation into a barotropic hydrodynamic model.

sion of the model, namely, GOT4.8, is based only on T/P satellite primary and interleaved mission data, without the use of Jason data in deep ocean areas. The enhancement over GOT4.7 is related to improvement in the processing of the dry tropospheric correction for altimeter data.

The OSU12 global ocean tide model was developed at the Ohio State University (Fok, 2012). It is a pure empirical tide model based on T/P, Jason-1/-2, Envisat and GFO satellite altimetry data that have been interpolated using least squares collocation onto a 0.25° × 0.25° grid. The covariance matrix used in this procedure varies from place to place and it depends on the depth of the ocean. Only diurnal and semidiurnal harmonics are provided.

The finite element solution (FES) tide model is a finite elements hydrodynamic model that assimilates tide gauge observations and multi-mission altimeter data (T/P, Jason-1, Jason-2, T/P interleaved, Jason-1 interleaved, ERS-1, ERS-2 and Envisat). The latest version of the FES, namely FES2014, is based on the resolution of the shallow water hydrodynamic equations in a spectral configuration and using a global finite element mesh with increasing resolution in coastal and shallow-water areas regions (Carrere et al., 2015).

The Hamburg direct data assimilation methods for TIDEs (HAMTIDE) tide model was developed at the Institute für Meereskunde of the University of Hamburg. It is based on the generalized inverse methods for tides developed at the same institute (Zahel, 1995). The dynamic residuals are used for the detection of possible model errors, e.g., bathymetry, parameterization of dissipation, loading and self-attraction (Taguchi et al., 2010).

The inverse tide model TPXO8 was developed at Oregon State University (Egbert and Erofeeva, 2002). It is the most recent in a series of tidal solutions produced to combine the efficient representer calculation scheme (Egbert et al., 1994) with programs for generating grids, boundary conditions, tidal forcing, dynamical error covariances, and altimetry datasets into a relocatable system for inverse barotropic tidal modelling. This model solution, which assimilates multi-mission satellite altimeter and tide gauge data, includes 13 tidal constituents. TPXO8 has a high-resolution grid of (1/30)° for nine global constituents and a low-resolution grid of (1/6)° for four additional constituents in coastal areas.

3 Methods

3.1 *Harmonic analysis method*

As one of the most widely used approach in tidal analysis, harmonic analysis determines the amplitude and phase of a priori known frequency via a least-squares fitting procedure. The tidal harmonic constants were obtained from the equation as follows (Godin, 1986):

$$\zeta(t) = h_0 + at + \sum_{i=1}^{n} f_i H_i \cos[\delta_i t + (V_0 + u)_i - g_i], \tag{1}$$

where h_0 is the mean sea surface height of the analysis data, a is the linear trend of the series, δ_i is the frequency of the ith tide component, V_{0i} is astronomy phase of the corresponding expanding term of tidal potential in Greenwich system of the ith tide component, f_i and u_i are nodal correction factors of the ith constituent, H_i and g_i are the amplitude and phase of the ith constituent, respectively, and n is the number of constituents. IB correction was applied to each tide gauge data to obtain the accurate tidal constituents.

IB correction was applied to each tide gauge data to obtain the accurate tidal constituents (Dorandeu and Le Traon, 1999). It was computed using mean sea level pressure from the monthly National Centers for Environmental Prediction/National Center for Atmospheric Research reanalysis data (Kalnay et al., 1996) provided by the National Oceanic and Atmospheric Administration (NOAA, https://www.esrl.noaa.gov/psd/data/reanalysis/reanalysis.shtml) with a spatial resolution of 2.5°×2.5°.

3.2 *Misfits between tide model and observation results*

The tidal constituents obtained from satellite altimetry and tide gauge data were used to compare with the corresponding tide model results.

To quantify each tidal constituent error between observation results and tide models, the root mean square (RMS) value was calculated using the following equation:

$$\mathrm{RMS} = \left\{ \frac{1}{2N} \sum_{i=1}^{N} [(H_0 \cos G_0 - H_m \cos G_m)^2 + (H_0 \sin G_0 - H_m \sin G_m)^2] \right\}^{\frac{1}{2}}, \tag{2}$$

where N is the number of points used, H_0 and G_0 are amplitude and phase obtained from observation data. Similarly, H_m and G_m are the corresponding amplitude and phase provided by tide models for the same tidal constituent.

The root sum square (RSS) value was also used to quantify the precision of each tide model, the RSS for the eight constituents was calculated by the following equation:

$$\mathrm{RSS} = \left(\sum_{j=1}^{M} \mathrm{RMS}_j^2 \right)^{\frac{1}{2}}, \tag{3}$$

where M is the eight tidal constituents mentioned above. It is important to note that all phases in this study are referred to as Greenwich Meridian Time.

4 Tidal constituent assessment

4.1 *Tidal constituents derived from altimetry and tide gauge data*

Eight major tidal constituents, namely, Q_1, O_1, P_1, K_1, N_2, M_2, S_2 and K_2 were extracted by harmonic analysis method to the long-term tidal height time series of tide gauge data. In this study, the T_TIDE tide analysis software package was employed to extract tidal constituents from tide gauge time series. T_TIDE is a package of routines that can be used to perform classical harmonic analysis with nodal corrections, inference, and a variety of user specified options (Pawlowicz et al., 2002). Although tide gauge observations containing time gaps, T_TIDE has the ability to analyze irregularly spaced time series. The amplitude and phase of K_1, O_1, M_2 and S_2 were listed in Table 1.

The amplitude and phase of diurnal (O_1, K_1) and semidiurnal (M_2, S_2) were shown in Figs. 2–5, which were extracted from the multi-mission satellite data. The satellite-derived tidal constituents were compared comprehensively with tide gauge observations in Fu et al. (2020), so that we have a better understanding of the areas where the tide calculated by altimeter is accurate. The tidal constants, whether amplitude or phase, vary more gently in the open ocean, and their magnitudes are more concentrated. However, in the shallow water area, the situation is just the opposite, and the change gradient is significant. Combine the influence of factors such as shoreline and water depth, there are several amphidromic points maybe in the Gulf of Thailand, the Taiwan Strait and the north-east of the SCS.

4.2 *Comparisons with satellite-derived results*

Satellite-derived tidal constituents were used to assess the accuracy of the seven tide models in the SCS. The model results were interpolated for the locations of the along-track points and then both the RMS and RSS values were calculated. The study area of the SCS was divided into a shallow-water area and a deep-water area using the depth of 200 m as the threshold. The shallow-water area was used to analyze the accuracy of the performance of the tide models.

RMS value of each tidal constituent and RSS value of the tide

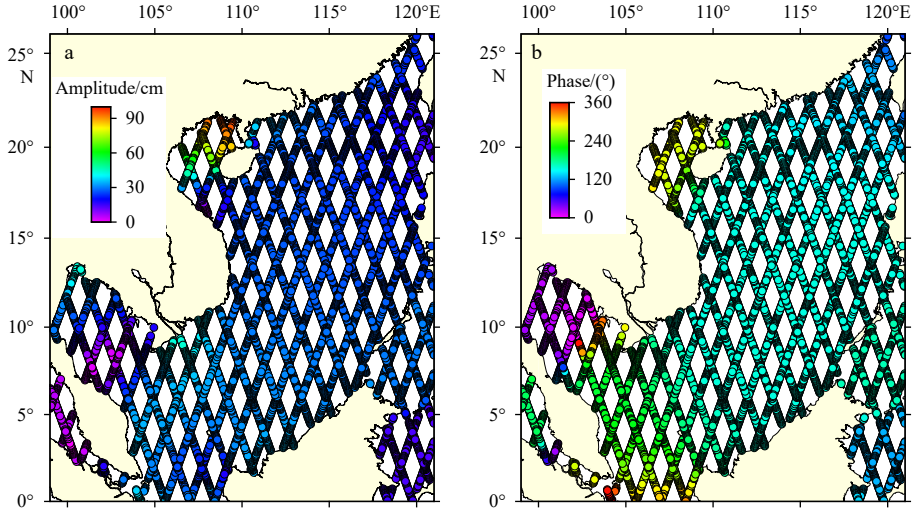

Fig. 2. Satellite-derived amplitude (a) and phase (b) of O_1 tidal constituents.

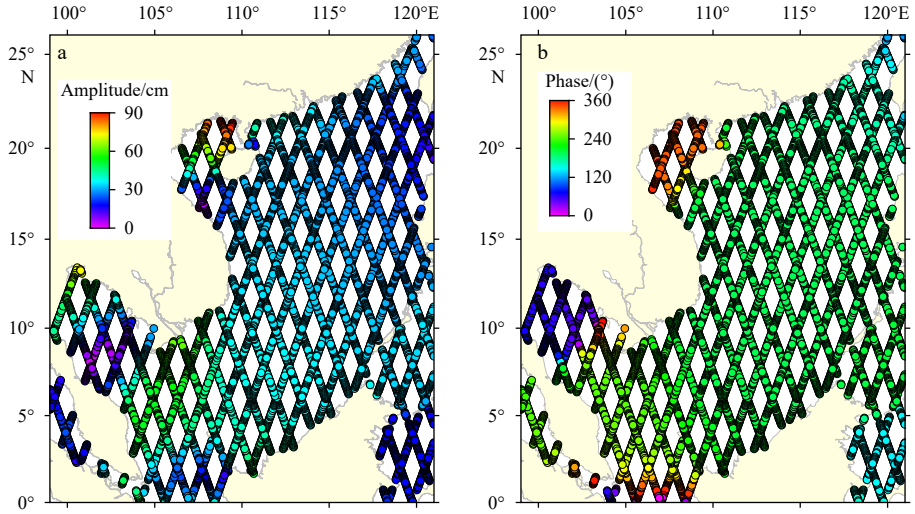

Fig. 3. Satellite-derived amplitude (a) and phase (b) of K_1 tidal constituents.

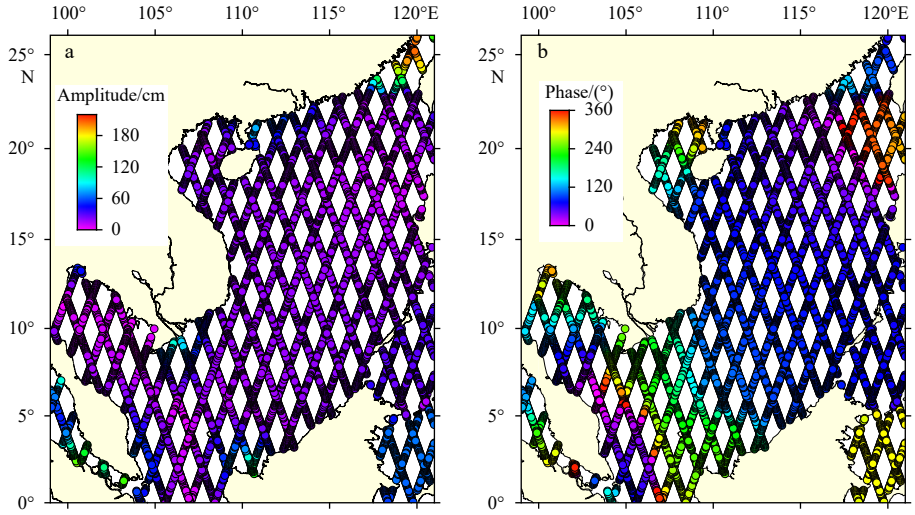

Fig. 4. Satellite-derived amplitude (a) and phase (b) of M_2 tidal constituents.

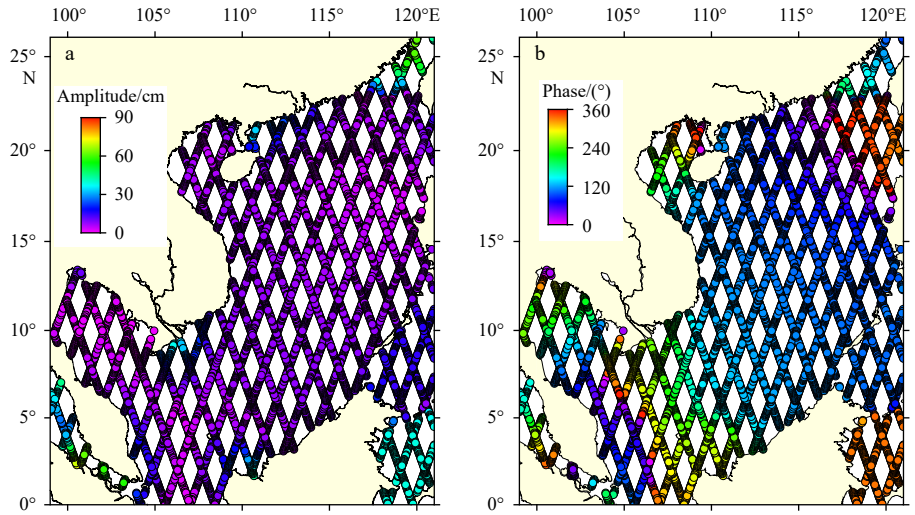

Fig. 5. Satellite-derived amplitude (a) and phase (b) of S_2 tidal constituents.

models are summarized in Table 3 for the entire SCS study area, and separately for the deep-water area (depth>200 m) and the shallow-water area (depth<200 m). The shallow-water area exhibited reasonably poor quality of tide prediction capability. This was primarily because of the large amplitude of the M_2 and K_1 constituents with differences of 1.90 cm and 1.55 cm in the deep water respectively, and of 5.63 cm and 4.14 cm in the shallow water, respectively. The remaining constituents had RMS values in the range of 0.72–1.26 cm in the deep water and 1.18–3.09 cm in the shallow water, respectively.

In general, the RMS value depend strongly on the tidal range of the study area. The M_2 constituent exhibited the largest order of amplitude in comparison with the other constituents in the SCS area. As expected, in the studied cases, the M_2 constituent had the largest RMS value. The distribution of the RMS value of the M_2 constituent for the seven tested tide models is illustrated in Fig. 6.

The spatial distribution of the RMS values of the seven tide models was very similar, with a difference of only a few millimeters between them for the open ocean. In shallow-water areas, the larger differences were distributed mainly in the Taiwan Strait (EOT11a and GOT4.8), Gulf of Thailand (EOT11a and HAMTIDE12), and Strait of Malacca (GOT4.8, HAMTIDE12, and TPXO8), where the average water depth is less than 100 m. The maximum RMS value of above 32 cm was found in the Strait of Malacca for HAMTIDE12. The Strait of Malacca is a highly com-

Table 3. RMS values between the tide models of the South China Sea and their RSS values

Water depth	Points number	RMS/cm								RSS/cm
		Q_1	O_1	P_1	K_1	N_2	M_2	S_2	K_2	
	8 376	0.97	2.19	1.39	3.08	1.28	4.14	2.29	1.11	6.51
<200 m	4 027	1.18	2.87	1.72	4.14	1.63	5.63	3.09	1.39	8.69
>200 m	4 349	0.72	1.26	0.99	1.55	0.84	1.90	1.13	0.78	3.42

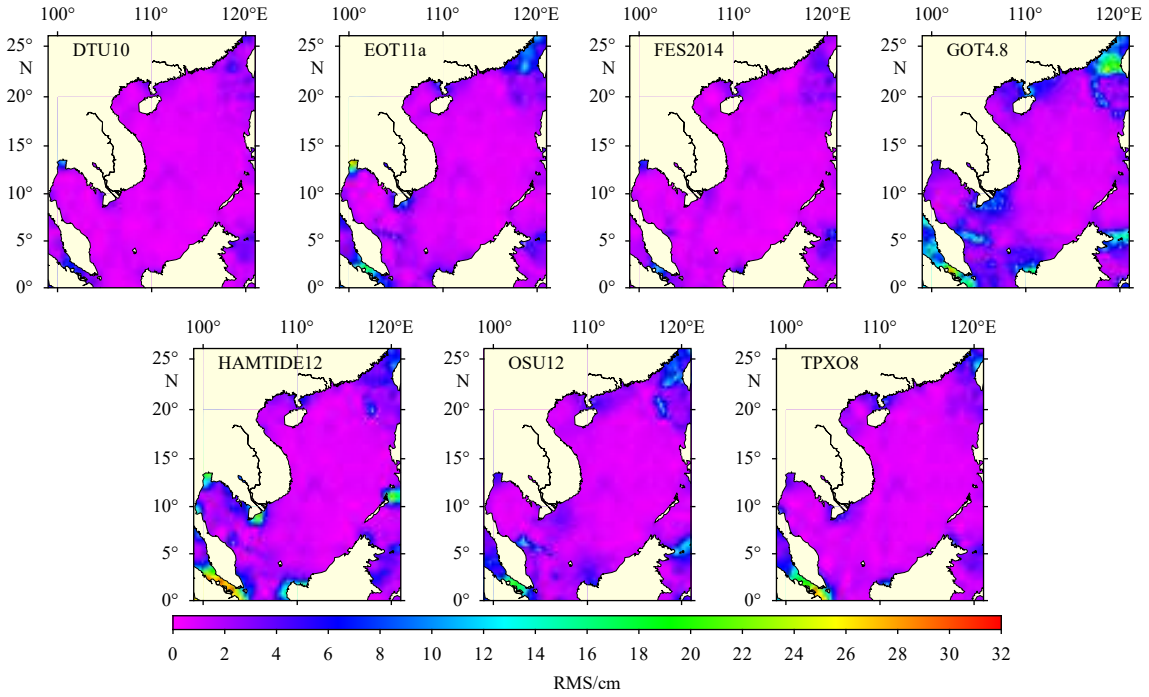

Fig. 6. Spatial distribution of RMS value for the M_2 tidal constituent.

plex hydrodynamic system. Tidal waves, especially the semidiurnal M_2 tidal component generated in the Indian Ocean (Rizal et al., 2012) and mixed diurnal and semidiurnal waves from the SCS, interact at the southern end of the Strait of Malacca and produce a high tidal range (Chen et al., 2005). The complicated dynamics along the Strait of Malacca affected the accuracy of HAMTIDE12, and in areas with sparse altimetry data, limited the accuracy of the empirical GOT4.8 and OSU12 models with coarse resolution of 0.5° and 0.25°, respectively.

Comparison of the model results in shallow-water areas was performed, instead of over the entire SCS domain, because shallow-water areas are where the models most need improvement. Table 3 presents the comparison results for eight tidal constituents in shallow-water areas (depth<200 m).

Little difference was found between the models, in terms of the RMS values of the Q_1, P_1, N_2 and K_2 constituents, i.e., the values ranged between 0.91 cm and 2.33 cm, with the performance of GOT4.8 found slightly the inferior. This was mainly because the overall averages were heavily weighted by the shallow-water points where accuracy is known to be good for all models, except for the above-mentioned straits areas. Four of the tide models, i.e., DTU10, EOT11a, FES2014 and TPXO8, showed the best performance in terms of accuracy (smallest RMS value) for at least one constituent (marked in bold in Table 4). DTU10 and FES2014 presented the most such entries, although the value for K_1 of DTU10 was slightly higher than FES2014 and the value for M_2 of FES2014 was slightly higher than DTU10. FES2014 exhibited the smallest RSS value of the seven tide models, indicating the best accuracy performance.

4.3 *Comparisons with tide gauge results*

The tide gauge data considered in this section were obtained from 37 stations (Fig. 1). Firstly, tidal height time series were used to evaluate the ability of the tidal model to predict tidal heights. The tide level predictions for the same time at each tide gauge station were made using the harmonic constants extracted by spline interpolation method from each tide model. Then, the predictions for the tide stations were compared with observations.

Comparisons between the predictions of each tide model and the tide gauge observations are shown in Fig. 7. Each panel presents the percentage of comparisons within ±10 cm and ±20 cm. It can be seen that the difference between most predictions and observations was in the range of ±50 cm, except the difference for GOT4.8 model was up to ±100 cm for some stations. Further-

Table 4. Comparison of satellite results and tide models in shallow-water areas

Tide model	RMS/cm								RSS/cm
	Q_1	O_1	P_1	K_1	N_2	M_2	S_2	K_2	
DTU10	**0.91**	**1.75**	**1.56**	2.16	**1.23**	**1.90**	**1.48**	**1.16**	**4.43**
EOT11a	**0.93**	2.27	1.66	3.89	1.43	4.22	2.53	**1.19**	7.18
FES2014	**0.92**	**1.22**	**1.32**	**1.82**	**1.10**	2.42	**1.39**	**1.03**	**4.18**
GOT4.8	1.27	3.65	2.11	5.15	2.33	6.51	3.72	1.63	10.50
HAMTIDE12	1.08	3.07	1.63	3.67	1.59	5.84	4.15	1.61	9.12
OSU12	1.48	2.94	1.79	4.16	1.65	4.22	3.08	1.43	7.96
TPXO8	1.45	**1.75**	**1.57**	2.31	1.43	3.82	2.59	1.23	6.15

Note: Bold values represent the best performance in terms of accuracy.

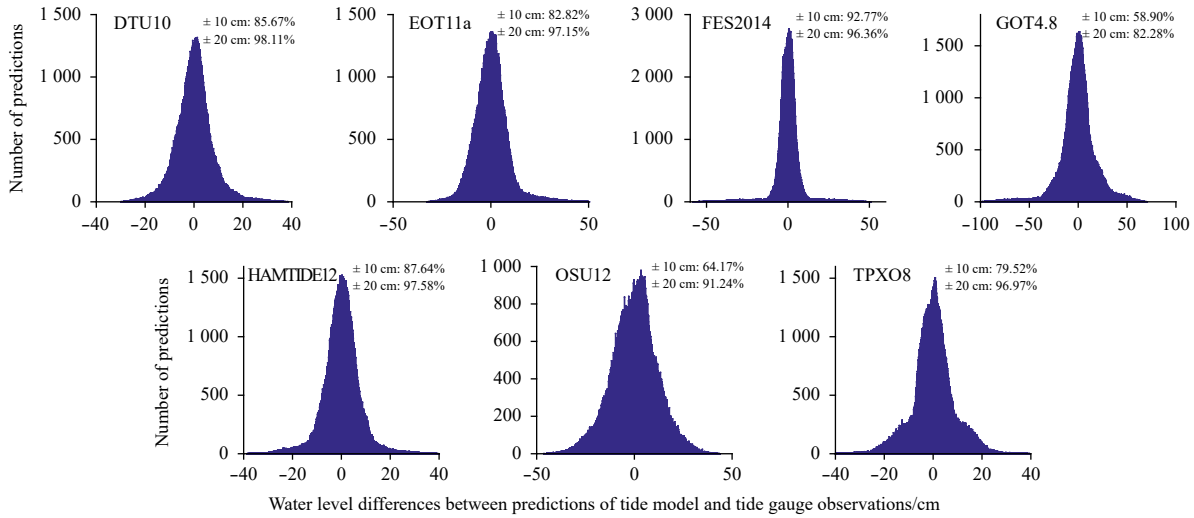

Fig. 7. Comparisons between predictions of each tide model and tide gauge observations.

more, the percentage of differences in the range of ±10 cm for FES2014 model was up to 92.77%, i.e., much larger than the other tide models. Thus, it can be assessed preliminarily that FES2014 can produce highly accurate prediction results for most tide stations.

Using the least-squares-based harmonic analysis method, the eight major tidal constituents mentioned above were extracted successfully with high accuracy through use of the long time series data. Comparison results for the seven tide models are listed in Table 5. As anticipated, the discrepancies between the tidal models and tide gauge observations were large for stations located in shallow-water areas or along the continental coastlines. The RMS values of the S_2, K_1 and O_1 major tidal constituents were found in the range of 2.79–7.45 cm; however, the RMS values for the M_2 constituent were in the range of 6.13–14.60 cm. The remaining constituents (i.e., N_2, K_2, Q_1 and P_1) had comparatively lower RMS values of 0.95–4.78 cm.

The RMS values between the tide gauge data and the tide models were influenced by the magnitude of the constituent amplitude. For example, the average amplitude value of the 37 tide gauges for M_2 and K_2 were 50.84 cm and 5.29 cm, respectively. The values of the amplitude and phase of the M_2 constituent at the Hon Dau station for the DTU10 model were 4.69 cm and 148.35° respectively, and the corresponding tide gauge results were 5.87 cm and 197.99°, respectively; however, the calculated RMS value was only 3.22 cm. For the Lumut station, the DTU10 model results of the amplitude and phase of the M_2 constituent were 59.34 cm and 226.57° respectively, and the tide gauge results were 74.47 cm and 241.51°, respectively; however, the RMS value was 16.25 cm. Therefore, it is misleading to suggest that K_2 had a lower RMS value than M_2, because the means of these tides are very different (~50–100 cm for M_2 at most stations, but likely ⩽5 cm for K_2 at most stations).

Combine the tidal constituents results provided by Fang et al., (1999) to assess the accuracy difference between FES2014 and HAMTIDE12, in which only four major tidal constants in 58 tide gauge stations were estimated. Histograms of the RMS values of M_2 between the 81 tide gauge results (there are 14 tide gauge stations overlapped for the both dataset) and two tide models (FES2014 and HAMTIDE12) are shown in Fig. 8. Both models were accurate for most stations with median RMS values ⩽3.65 cm. Overall, there were 70.24% and 61.90% of stations with RMS values ⩽5 cm for FES2014 and HAMTIDE12 model results, respectively; however, some stations had larger RMS values that would skew an RMS statistic. It was found that FES2014 had poor agreement at two stations, while HAMTIDE12 had poor performance at three stations. The RMS statistics of M_2 and RSS values were dominated by a few stations with large model errors. Therefore, most of the tide models were found reasonably accurate for the majority of tide gauge stations; however, large errors were found to occur in a few locations.

5 Discussion

The discrepancy of each tide model in tidal estimation over the shallow water and coastal zones of the SCS was large. Overall, the model with better performance was found to be FES2014. This model shows RSS value of 9.35 cm when compared with tide gauge results around the SCS region, this is mainly due to, apart

Table 5. RMS and RSS values between the models and the 37 tide gauge stations

Tide model	RMS/cm								RSS/cm
	Q_1	O_1	P_1	K_1	N_2	M_2	S_2	K_2	
DTU10	1.52	7.12	2.32	5.96	1.97	9.92	5.42	1.90	15.14
EOT11a	0.95	3.59	1.47	4.20	2.77	10.11	6.07	2.12	13.59
FES2014	1.04	4.08	2.14	3.96	1.46	6.13	2.79	1.42	9.35
GOT4.8	1.30	5.89	2.11	6.02	2.70	11.99	4.79	2.29	16.01
HAMTIDE12	1.38	7.44	1.66	6.12	4.78	13.30	7.45	3.53	19.11
OSU12	1.46	5.58	1.66	4.89	4.28	8.19	5.36	2.41	13.41
TPXO8	1.23	5.36	1.91	3.82	3.16	14.60	7.41	2.62	18.26

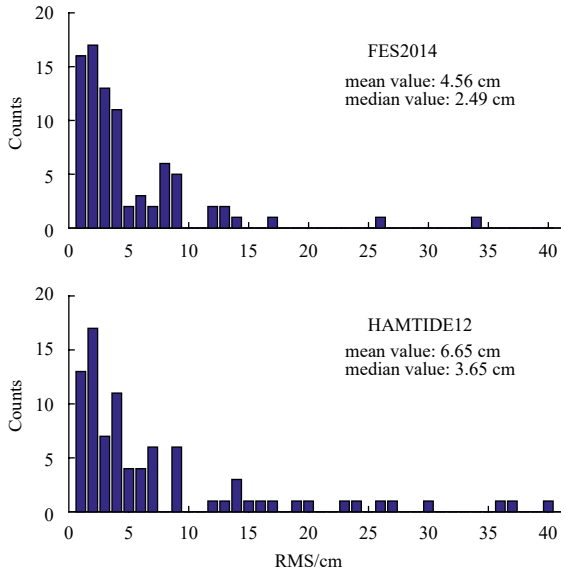

Fig. 8. Histograms of RMS values in M_2 between the 84 tide gauge stations and FES2014 and HAMTIDE12. Overall, 54.76% (FES 2014) and 44.05% (HAMTIDE12) of stations agreed with the corresponding model to accuracy better than 3 cm.

from data assimilation, taking advantage of datasets with improved accuracy derived from long altimeter time series and enhanced altimeter standards, the resolution of the shallow water hydrodynamic equations in a spectral configuration is based and using a global finite element mesh with increasing resolution in coastal and shallow-water areas regions.

In shallow water areas of the SCS, the difference of spatial distribution of each empirical tide model is small. This is mainly due to the different satellite data were used to establish the models. The accuracy performance of GOT4.8 in the Strait of Malacca is poor than other models (Fig. 6) because it is based only on T/P satellite primary and interleaved mission data, without the use of Jason data, but others such as OSU12 based on T/P, Jason-1/-2, Envisat and GFO satellite altimetry data. Furthermore, different approaches about the residual tidal analysis may cause ~2 cm of RMS difference in each tidal constant when compared with satellite along-track results (Table 4). For example, DTU10 applies response method to the residual tide analysis and uses the dynamic interpolation method to perform interpolation of the along-track data to the FES2004 grid, as such, it can be seen that accuracy of the DTU10 (i.e., RSS value is 4.43 cm) is much higher than other empirical models. However, subject to a series of factors, such as the bathymetry data, bottom friction and open boundary condition, the accuracy of the hydrodynamic models is regional different. HAMTIDE12 and TPXO8 have similar accuracy performance over the whole SCS area. The slight poor accuracy in the Strait of Malacca of HAMTIDE12 lead to its low RSS values in the shallow water areas.

In coastal zones of the SCS, many factors affect the accuracy of tide models when compared with tide gauge observations. Tidal height obtained by tide gauge is the relative sea level change, which is mainly affected by vertical land movement. As such, the major tide is varying when extracted from tide gauge observations with different length of tidal height tide series or different time span. For example, the differences in the tidal constants obtained from the interannual time series are at the centimeter level. It is worthy note that most tide gauge stations are located in the coastal regions, the different resolutions of tide models make the extracted tidal constants by different interpolation methods are also different. For example, GOT4.8 is distributed as a set of tidal harmonic constants on a 0.5° × 0.5° grid. However, the grid does not extend to the shoreline ubiquitously, which may be the cause of poor accuracy in tidal constituents in coastal zone.

6 Conclusions

Based on a comparison of tidal constituents obtained from satellite altimetry and tide gauge data, the accuracy of seven global ocean tide models (DTU10, EOT11a, FES2014, GOT4.8, HAMTIDE12, OSU12 and TPXO8) was assessed in the SCS. As expected, tide models exhibit high precision in deep-water areas, where the RMS values of tidal constituents were found in the range of 0.72–1.90 cm. The accuracy performance of those tide models in the shallow water area (depth<200 m) and coastal zones was investigated from the satellite-derived and tide gauge observations.

Compared with the multi-mission satellite-derived tidal constituents in the shallow water areas, the tide models represented similar spatial patterns with the RSS value in the range of 4.18–10.50 cm. FES2014 and DTU10 models showed slightly prior accuracy performance. The possible reasons for the model differences were discussed. The comparison results between tide models and tide gauge station data showed that the RSS values for eight major tidal constituents were found in the range of 9.35–19.11 cm. It was also established that the FES2014 model had the best performance. The time variability of tidal constants obtained from tide gauge observations and the interpolation mode of tide models with varies spatial resolution are the possible reasons for the differences between models.

Acknowledgements

Satellite altimetry data used in this study were developed, validated, and distributed by the CTOH/LEGOS, France. We acknowledge the CTOH for providing the satellite-derived harmonic constants of tidal constituents, PSMSL for providing the tide gauge data, and NOAA for providing the IB correction data.

References

Amante C, Eakins B W. 2009. ETOPO1 1 arc-minute global relief model: procedures, data sources and analysis. In: National Oceanic and Atmospheric Administration. NOAA Technical Memorandum NESDIS NGDC-24. Boulder, Colorado: National Geophysical Data Center, NOAA, 1–19, doi: 10.7289/V5C8276M

Andersen O B, Woodworth P L, Flather R A. 1995. Intercomparison of recent ocean tide models. Journal of Geophysical Research: Oceans, 100(C12): 25261–25282, doi: 10.1029/95JC02642

Carrere L, Lyard F, Cancet M, et al. 2015. FES 2014, a new tidal model on the global ocean with enhanced accuracy in shallow seas and in the Arctic region. In: EGU General Assembly 2015. Vienna, Austria: EGU

Chen Ming, Murali K, Khoo B C, et al. 2005. Circulation modelling in the strait of Singapore. Journal of Coastal Research, 21(5): 960–972

Cheng Yongcun, Andersen O B. 2011. Multimission empirical ocean tide modeling for shallow waters and polar seas. Journal of Geophysical Research: Oceans, 116(C11): C11001, doi: 10.1029/2011JC007172

Cheng Yongcun, Xu Qing, Zhang Yuan. 2016. Tidal estimation from TOPEX/Poseidon, Jason primary, and Interleaved missions in the Bohai, Yellow, and East China seas. Journal of Coastal Research, 32(4): 966–973, doi: 10.2112/JCOASTRES-D-14-00209.1

Cherniawsky J Y, Foreman M G G, Crawford W R, et al. 2001. Ocean

tides from TOPEX/Poseidon sea level data. Journal of Atmospheric and Oceanic Technology, 18(4): 649–664, doi: 10.1175/1520-0426(2001)018<0649:OTFTPS>2.0.CO;2

Daher V B, de Oliveira Vieira Paes R C, França G B, et al. 2015. Extraction of tide constituents by harmonic analysis using altimetry satellite data in the Brazilian coast. Journal of Atmospheric and Oceanic Technology, 32(3): 614–626, doi: 10.1175/JTECH-D-14-00091.1

Desportes E, Obligis E, Eymard L. 2007. On the wet tropospheric correction for altimetry in coastal regions. IEEE Transactions on Geoscience and Remote Sensing, 45(7): 2139–2149, doi: 10.1109/TGRS.2006.888967

Dorandeu J, Le Traon P Y. 1999. Effects of global mean atmospheric pressure variations on mean sea level changes from TOPEX/Poseidon. Journal of Atmospheric and Oceanic Technology, 16(9): 1279–1283, doi: 10.1175/1520-0426(1999)016<1279:EOGMAP>2.0.CO;2

Egbert G D, Bennett A F, Foreman M G G. 1994. TOPEX/POSEIDON tides estimated using a global inverse model. Journal of Geophysical Research: Oceans, 99(C12): 24821–24852, doi: 10.1029/94JC01894

Egbert G D, Erofeeva S Y. 2002. Efficient inverse modeling of barotropic ocean tides. Journal of Atmospheric and Oceanic Technology, 19(2): 183–204, doi: 10.1175/1520-0426(2002)019<0183:EIMOBO>2.0.CO;2

Egbert G D, Ray R D. 2000. Significant dissipation of tidal energy in the deep ocean inferred from satellite altimeter data. Nature, 405(6788): 775–778, doi: 10.1038/35015531

Fang Guohong. 1986. Tide and tidal current charts for the marginal seas adjacent to China. Chinese Journal of Oceanology and Limnology, 4(1): 1–16, doi: 10.1007/BF02850393

Fang Guohong, Kwok Y K, Yu Kejun, et al. 1999. Numerical simulation of principal tidal constituents in the South China Sea, Gulf of Tonkin and Gulf of Thailand. Continental Shelf Research, 19(7): 845–869, doi: 10.1016/S0278-4343(99)00002-3

Fok H S, Iz H B, Shum C K, et al. 2010. Evaluation of ocean tide models used for Jason-2 altimetry corrections. Marine Geodesy, 33(S1): 285–303, doi: 10.1080/01490419.2010.491027

Fok H S. 2012. Ocean tides modeling using satellite altimetry [dissertation]. Columbus, OH, USA: The Ohio State University

Fu Yanguang, Zhou Dongxu, Zhou Xinghua, et al. 2020. Evaluation of satellite-derived tidal constituents in the South China Sea by adopting the most suitable geophysical correction models. Journal of Oceanography, 76: 183–196, doi: 10.1007/s10872-019-00537-2

Fu L L, Cazenave A. 2001. Satellite Altimetry and Earth Sciences: A Handbook of Techniques and Applications. San Diego: Academic Press, 463

Godin G. 1986. The use of nodal corrections in the calculation of harmonic constants. International Hydrographic Review, 63(2): 143–162

Green J A M, David T W. 2013. Non-assimilated tidal modeling of the South China Sea. Deep -Sea Research Part I: Oceanographic Research Papers, 78: 42–48, doi: 10.1016/j.dsr.2013.04.006

Groves G W, Reynolds R W. 1975. An orthogonalized convolution method of tide prediction. Journal of Geophysical Research, 80(30): 4131–4138, doi: 10.1029/JC080i030p04131

Iliffe J C, Ziebart M K, Turner J F, et al. 2013. Accuracy of vertical datum surfaces in coastal and offshore zones. Survey Review, 45(331): 254–262, doi: 10.1179/1752270613Y.0000000040

Kalnay E, Kanamitsu M, Kistle R, et al. 1996. The NCEP/NCAR 40-year reanalysis project. Bulletin of the American Meteorological Society, 77(3): 437–472, doi: 10.1175/1520-0477(1996)077<0437:TNYRP>2.0.CO;2

Keysers J H, Quadros N D, Collier P A. 2015. Vertical datum transformations across the Australian littoral zone. Journal of Coastal Research, 31(1): 119–128, doi: 10.2112/JCOASTRES-D-12-00228.1

Lyard F, Lefevre F, Letellier T, et al. 2006. Modelling the global ocean tides: modern insights from FES2004. Ocean Dynamics, 56(5–6): 394–415, doi: 10.1007/s10236-006-0086-x

Mayer-Gürr T, Savcenko R, Bosch W, et al. 2012. Ocean tides from satellite altimetry and GRACE. Journal of Geodynamics, 59–60: 28–38, doi: 10.1016/j.jog.2011.10.009

Munk W H, Cartwright D E. 1966. Tidal spectroscopy and prediction. Philosophical Transactions of the Royal Society A: Mathematical, Physical and Engineering Sciences, 259(1105): 533–583, doi: 10.1098/rsta.1966.0024

Pawlowicz R, Beardsley B, Lentz S. 2002. Classical tidal harmonic analysis including error estimates in MATLAB using T_TIDE. Computers & Geosciences, 28(8): 929–937, doi: 10.1016/S0098-3004(02)00013-4

Ray R D. 1999. A global ocean tide model from TOPEX/POSEIDON altimetry, GOT99.2. In: NASA/TM—1999-209478. Greenbelt, MD: Goddard Space Flight Center, 58

Rizal S, Damm P, Wahid M A, et al. 2012. General circulation in the Malacca Strait and Andaman Sea: a numerical model study. American Journal of Environmental Sciences, 8(5): 479–488, doi: 10.3844/ajessp.2012.479.488

Savcenko R, Bosch W. 2012. EOT11a-Empirical ocean tide model from multi-mission satellite altimetry. Munchen: Deutsches Geodätisches Forschungsinstitut (DGFI), 89, 49, https://epic.awi.de/id/eprint/36001/1/DGFI_Report_89.pdf [2017-11-8]

Schrama E J O, Ray R D. 1994. A preliminary tidal analysis of TOPEX/POSEIDON altimetry. Journal of Geophysical Research: Oceans, 99(C12): 24799–24808, doi: 10.1029/94JC01432

Seifi F, Deng Xiaoli, Andersen O B. 2019. Assessment of the accuracy of recent empirical and assimilated tidal models for the Great Barrier Reef, Australia, using satellite and coastal data. Remote Sensing, 11(10): 1211, doi: 10.3390/rs11101211

Shum C K, Woodworth P L, Andersen O B, et al. 1997. Accuracy assessment of recent ocean tide models. Journal of Geophysical Research: Oceans, 102(C11): 25173–25194, doi: 10.1029/97JC00445

Stammer D, Ray R D, Ander O B, et al. 2014. Accuracy assessment of global barotropic ocean tide models. Reviews of Geophysics, 52(3): 243–282, doi: 10.1002/2014RG000450

Taguchi E, Stammer D, Zahel W. 2010. Inferring deep ocean tidal energy dissipation from the global high-resolution data-assimilative HAMTIDE model. Journal of Geophysical Research: Oceans, 119(7): 4573–4592, doi: 10.1002/2013JC009766

Visser P N A M, Sneeuw N, Reubelt T, et al. 2010. Space-borne gravimetric satellite constellations and ocean tides: aliasing effects. Geophysical Journal International, 181(2): 789–805, doi: 10.1111/j.1365-246X.2010.04557.x

Ye A L, Robinson I S. 1983. Tidal dynamics in the South China Sea. Geophysical Journal International, 72(3): 691–707, doi: 10.1111/j.1365-246X.1983.tb02827.x

Zahel W. 1995. Assimilating ocean tide determined data into global tidal models. Journal of Marine Systems, 6(1–2): 3–13, doi: 10.1016/0924-7963(94)00014-3

Zu Tingting, Gan Jianping, Erofeeva S Y. 2008. Numerical study of the tide and tidal dynamics in the South China Sea. Deep-Sea Research Part I: Oceanographic Research Papers, 55(2): 137–154, doi: 10.1016/j.dsr.2007.10.007